

Accepted Article

Title: Organic Chimeras Based on Selenosugars, Steroids, and Fullerenes as Potential Inhibitors of the β -amyloid Peptide Aggregation

Authors: Reinier Lemos, Yoana Pérez-Badell, Mauro De Nisco, Andrea Carpentieri, Margarita Suárez, and Silvana Pedatella

This manuscript has been accepted after peer review and appears as an Accepted Article online prior to editing, proofing, and formal publication of the final Version of Record (VoR). The VoR will be published online in Early View as soon as possible and may be different to this Accepted Article as a result of editing. Readers should obtain the VoR from the journal website shown below when it is published to ensure accuracy of information. The authors are responsible for the content of this Accepted Article.

To be cited as: *ChemPlusChem* **2024**, e202400404

Link to VoR: <https://doi.org/10.1002/cplu.202400404>

RESEARCH ARTICLE

Organic Chimeras Based on Selenosugars, Steroids, and Fullerenes as Potential Inhibitors of the β -amyloid Peptide Aggregation

Reinier Lemos,^[a,b] Yoana Pérez-Badell,^[c] Mauro De Nisco,^[d] Andrea Carpentieri,^[b] Margarita Suárez,^{*[a]} Silvana Pedatella^{*[b]}

[a] Dr. R. Lemos, Prof. Dr. M. Suárez

Laboratorio de Síntesis Orgánica
Facultad de Química, Universidad de la Habana
10400-La Habana, Cuba
E-mail: msuarez@fq.uh.cu

[b] Dr. R. Lemos, Prof. Dr. A. Carpentieri, Dr. S. Pedatella

Dept. of Chemical Sciences
University of Napoli Federico II
Via Cintia 4, I-80126 Napoli, Italy
Email: pedatell@unina.it

[c] Dr. Y. Perez-Badell

Laboratorio de Química Computacional y Teórica
Facultad de Química, Universidad de La Habana
10400-La Habana, Cuba

[d] Dr. Mauro De Nisco

Dept. of Chemical Sciences
University of Basilicata
Viale dell'Ateneo Lucano 10, I-85100 Potenza, Italy

Supporting information for this article is given via a link at the end of the document.

Abstract: The aggregation of β -amyloid peptide ($A\beta$) is associated with neurodegenerative diseases such as Alzheimer's disease (AD). Several therapies aimed at reducing the aggregation of this peptide have emerged as potential strategies for the treatment of AD. This paper describes the design and preparation of new hybrid molecules based on steroids, selenosugars, and [60]fullerene as potential inhibitors of $A\beta$ oligomerization. These moieties were selected based on their antioxidant properties and possible areas of interaction with the $A\beta$. Cyclopropanations between C_{60} and malonates bearing different steroid and selenosugar moieties using the Bingel–Hirsch protocol have enabled the synthesis of functionalized molecular hybrids. The obtained derivatives were characterized by physical and spectroscopic techniques. Theoretical calculations for all the selenium compounds were performed using the density functional theory DFT/B3LYP-D3(BJ)/6-311G(2d,p) predicting the most stable conformations of the synthesized derivatives. Relevant geometrical parameters were investigated to relate the stereochemical behavior and the spectroscopic data obtained. The affinity of the compounds for $A\beta$ -peptide was estimated by molecular docking simulation, which predicted an increase in affinity and interactions for $A\beta$ for the hybrids containing the C_{60} core. In addition, parameters such as lipophilicity, polar surface area, and dipole moment were calculated to predict their potential interaction with membrane cells.

Introduction

The formation of amyloid fibrillar aggregates by the auto-aggregation of peptides and proteins constitute neuropathological structures of several diseases associated with neurodegenerative disorders (ND).^[1,2] These include Huntington's disease,^[3] Parkinson's disease,^[4] and Alzheimer's disease (AD),^[5] among others. In the early stages of AD, patients develop β -amyloid peptide ($A\beta$) aggregates in the hippocampus and other areas of the cerebral cortex involved in thinking and decision-making.^[6] An increase in the concentration of $A\beta$ and an accumulation of $A\beta$ aggregates causes neuronal death and loss of synapses in neurons, favoring the progression of cognitive decline.^[7] Several treatment strategies target the $A\beta$,^[8] one of which has been to reduce $A\beta$ production by inhibiting producing enzymes.^[9] However, these approaches have not led to significant cognitive improvements. Another implementation to decrease $A\beta$ aggregation in the brain is through molecules with a high affinity for the peptide or the ability to degrade it.^[10,11] The self-assembly of $A\beta$ monomers into amyloid fibrils is a complex multistep process, involving the formation of soluble oligomers, protofibrils, and insoluble mature fibrils.^[12] The presence of external factors such as carbon nanoparticles, metal ions, and small molecules can limit the aggregation process of $A\beta$. Among carbon nanoparticles, those based on fullerenes have been one of the most studied, due to the greater possibility of functionalization and chemical hybridization compared to

RESEARCH ARTICLE

graphite and nanotubes. Fullerenes, such as C₆₀ and its derivatives have remarkable anti-amyloid properties for AD and other neurodegenerative diseases.^[13] Furthermore, their ability to capture radicals makes them good antioxidants, for developing potential drugs to treat neurodegenerative diseases.^[14] Fullerene derivatives with solubilizing addends showed a strong anti-amyloid activity by interaction with the A β and by destruction of their aggregates. Toshima et al. have synthesized hybrid fulleropyrrolidines as protein-photodegradation agents and inhibitors of the cytotoxic A β in neuron-like PC12.^[15] Furthermore, amphipathic potassium fullereneolates polyadducts showed a strong anti-amyloid effect in vitro with A β and low cytotoxicity. Hydrophobic (fullerene) and hydrophilic (carboxylate) groups favor self-aggregation in water and produce stable supramolecular systems with hydrodynamic diameters less than 10 nm.^[16] Theoretical studies based on molecular docking and molecular dynamics show how fullerene prevents the aggregation of the A β for the strong hydrophobic and aromatic-stacking interactions. The hexagonal rings display a T-shape and π - π interaction with the aromatic rings of Phe residues. This C₆₀-Phe interaction could decrease the formation of the Phe-Phe interaction, one of the most important interactions reported in the aggregation of the A β peptide.^[17]

On the other hand, it has been described that steroids have a neuroprotective effect on the brain.^[18] Their biological properties are fundamentally due to their function as hormones in mammals and the regulation of other metabolic processes.^[19] In the case of Alzheimer's disease, steroid therapies have a preventive effect on the pathology and good results at the early onset of symptoms.^[20] Cholesterol is a precursor molecule of steroid hormones and bile acids, its presence in the brain has been related to the mechanisms of neurodegenerative diseases.^[21] The non-functionalized cholesterol can interact with biological receptors through a polar area (OH group), the sterane rings (CH- π stacking with aromatic residues),^[22] and an *iso*-octyl group capable of interacting or intercalating with apolar residues as Val, Leu, or Ile.^[23] However, this sterol can promote the aggregation and insertion of A β in the plasma membrane and prevent their cytotoxic.^[24] Experimental and theoretical studies suggest that the cholesterol-binding domain in the A β is in the 22-35 amino acid residue region. The main amino acids involved in the interaction of cholesterol are Val-24, Lys-28, and Ile-32.^[25] Therefore, molecules that can occupy the cholesterol-binding site of A β could potentially interfere with the aggregation and amyloid pore formation.^[21]

It has also been found that diosgenin, a spirostane steroid of natural origin, is a potential curative natural drug for AD.^[26] Diosgenin can penetrate cells through membrane-associated rapid response steroid-binding receptors^[27] and can restore A β -induced axonal atrophy in neurons and improve memory function in a mouse model.^[28] Diosgenin delivery has enhanced spatial learning and memory in animal studies and protected altered cognitive functions induced by A β . Furthermore, the biochemical analysis showed that this steroid decreased the aggregation of A β , oxidative stress, and neuroinflammation.^[29] Likewise, estradiol regulates A β accumulation in the brain, cell apoptosis, and the inhibition of excitotoxic neuronal death. Moreover, this estrogen is

involved in the inhibition of the hyperphosphorylation of Tau protein, a characteristic of Alzheimer's disease.^[18]

Another class of molecules widely studied for the treatment of neurodegenerative diseases are organoselenium derivatives. Several Se-containing compounds have been synthesized, and they turned out to be potent neuroprotective agents with a modest effect on normal tissues and are clinically well tolerated.^[30] One strategy to incorporate Se into the brain would be to synthesize different sugar molecules containing selenium in their structure. Selenosugars are well-known as drug carriers in the brain because they can be recognized by glucose receptors and transporters. The use of Se-containing molecules, with potential antioxidant properties, as drugs in the treatment of ND is, however, limited by the difficulty of crossing the blood-brain barrier (BBB). This problem can be solved by the conjugation of selenosugars to biomolecules such as steroids, which in addition to regular metabolic processes are well-known powerful biological transporters in drug design.^[31]

Most natural steroids have hydroxyl or carbonyl groups in different positions of their structure, which can be replaced by other functional groups.^[32] These structural features allow them to be functionalized, either by chemical means or by biological processes with the use of enzymes^[33] it is what makes the steroids attractive as platforms for the design and synthesis of more complex molecules. Our research group has reported the synthesis of hybrid molecules that take advantage of the properties of steroids to increase the biocompatibility of fullerenes as well as their solubility.^[34] Furthermore, we have recently developed hybrid systems that combine the properties of steroids and fullerenes with monosaccharides, in search of molecules with affinity for biological receptors and viral proteases.^[35]

Density-functional theory (DFT) calculations have proven to be important tools in the determination of the properties and reactivity of organo-selenium compounds.^[36] It represents the most widely used quantum-mechanical method for molecular-level computational research used in chemistry and physics to calculate the electronic structure of many-body systems with huge numbers of electrons.^[37] This knowledge, obtained through DFT calculations, can lead to a deeper understanding of these systems, including their practical applications.

It is well-known that the Bingel-Hirsch cyclopropanation protocol^[38] is an efficient methodology to generate functional entities in which each moiety modulates the properties and increases the solubility of the final compounds. This synthetic procedure constitutes one of the most widely applied reactions in fullerene's chemistry, due to its good selectivity and feasibility of adding a wide range of addends and functional groups.

In continuation of our interest in the chemistry of fullerene hybrids decorated with molecules of biological interest, here we report on the design of a new type of hybrid systems that combine the antioxidant and the A β anti-aggregation properties of steroids, the [60]fullerene, and selenosugars as potential molecules for the treatment of ND by the so-called Bingel-Hirsch reaction. In addition, theoretical calculations at the DFT-B3LYP-D3(BJ)/6-311G(2d,p) level of the synthesized conjugates predict the most stable conformation and determine the factors that control the hybrid molecules' geometry. Besides, molecular docking was

RESEARCH ARTICLE

carried out to estimate the potential application of the hybrids as A β aggregation inhibitors. Also, some stereoelectronic parameters were calculated to determine the electronic interactions present in these hybrid molecules.

Results and Discussion

The hybrid molecules reported in this work were based on the hydrophobic, polar, and π - π stacking interactions with the A β and the antioxidant character of the different moieties present in the structure. The structure of A β and interaction zones are represented in Figure 1 (A). Cholesterol, diosgenin, and estradiol were used as steroids to evaluate the potential influence of

different functional groups on the interaction with the A β using cholesterol as a model. Selenium was introduced into the conjugates in the form of selenosugars, which in addition to their known antioxidant character, constitute a polar region with electron donor groups in the conjugate. The antioxidant capacity of selenoglyconjugates containing the selenosugars derived from ribose used in the article has been experimentally verified in our group.^[39] Also, the presence of C₆₀ in these molecules would increase the affinity of the conjugates by hydrophobic and π - π stacking interactions. Therefore, two families of compounds were designed, see Figure 1 (B). A malonic acid derivative was used to conjugate selenosugars and steroid moieties. This is a linker able to easily functionalize the malonic moiety with the C₆₀ by a cyclopropanation reaction.

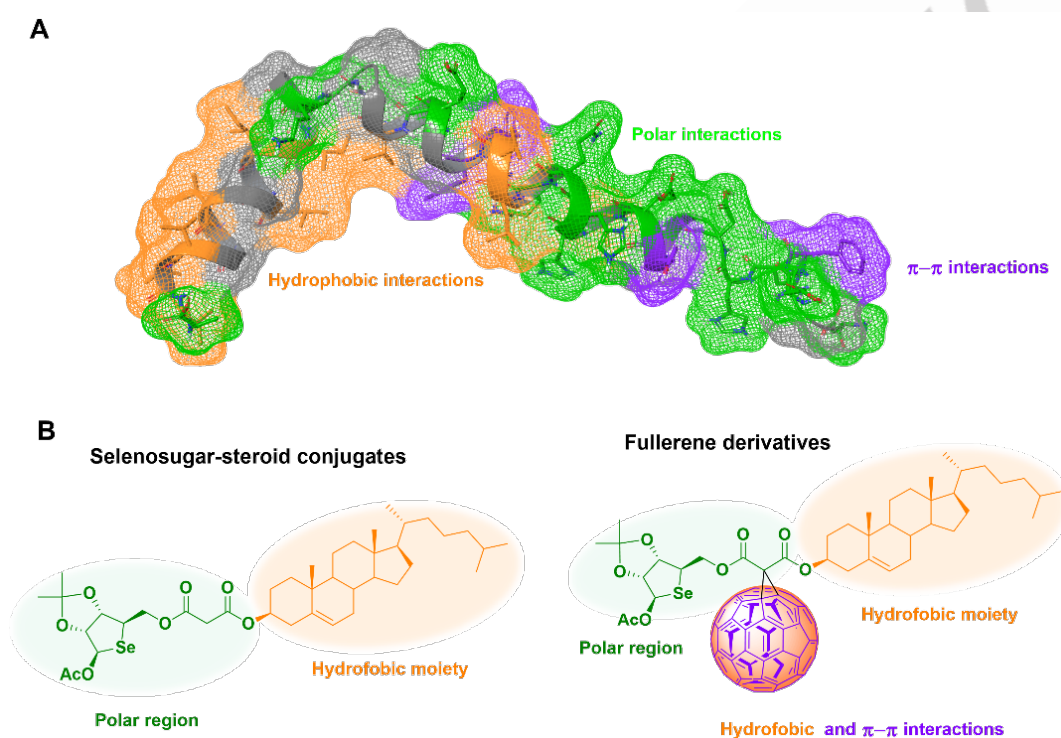


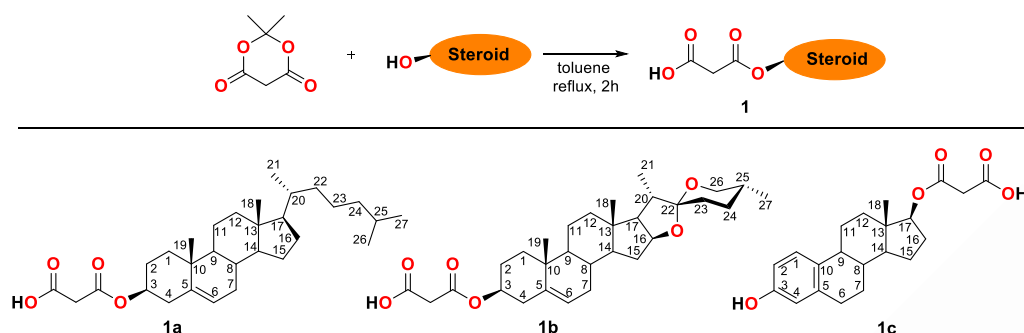
Figure 1. Design strategy for the synthesis of conjugates that can interact with the A β . (A) 3D Molecular model of A β ₁₋₄₂ peptide. The color surface represents the residues that present hydrophobic (orange), polar (green), and π - π (purple) interactions. (B) Representative structures of steroid-selenosugar conjugates and fullerene derivatives. The color indicates the potential region of interaction with the A β ₁₋₄₂ peptide.

Therefore, in the first step, we carried out the preparation of the required starting malonates (**1a-1c**) by treatment of three different sterols – cholesterol, diosgenin, and estradiol – with commercially available Meldrum acid (Scheme 1) taking into account the methodology developed by our research group.^[35]

The yields obtained with this method varied according to the steroid employed, so that oxopropanoic acids **1a** and **1b**, previously synthesized from diosgenin and cholesterol,^[35] were obtained with 86% and 85%, respectively, from steroids with hydroxyl groups at the C3 position. In the case of oxopropanoic acid derived from estradiol, the yield obtained was lower, 70%. Estradiol has two hydroxyl groups, one at C17 and one phenolic

hydroxyl group at C3. Under reaction conditions, the less nucleophilic nature of the phenolic group favors functionalization by the alcohol function. Despite the higher reactivity of the hydroxyl on C17, the decrease in yield of **1c** could be related to the steric hindrance caused by the axial methyl group (C18) and the detection of the formation of trace amounts of the functionalization product by the phenolic function. Although the phenolic functional group could be selectively protected, the results obtained are good enough, and additional protection and deprotection steps are avoided. The structure of the malonyl-steroids has been confirmed by both physical and spectroscopic data (see the Supporting Information).

RESEARCH ARTICLE

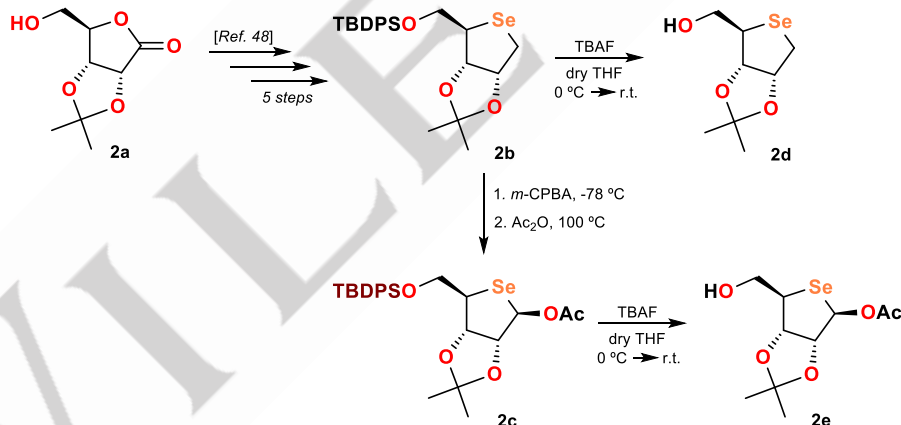


Scheme 1. Synthesis of malonyl steroids (**1**). Steroid: cholesterol (**a**), diosgenin (**b**), and estradiol (**c**).

Different methods for the synthesis of seleno-derivatives have been described in the literature. These include heterocyclic compounds^[40] and biomolecules.^[41] Based on this background and the strategies for transporting selenium to the brain, two selenium sugars (**2d** and **2e**) have been synthesized to be conjugated with the malonyl steroids. The synthesis of the selenium-containing compounds is represented in Scheme 2.

To conjugate the selenium scaffold with polyphenolic motifs, we previously reported the synthesis of **2d** via a multi-step synthetic route from **2a**.^[42] This procedure was employed to obtain the acetylated derivative **2e**. It was interesting to introduce an acetyl group in **2b** to obtain a pseudoanomeric carbon analogous to that of monosaccharides. The transformation was carried out by

oxidation with *m*-chloroperbenzoic acid (*m*-CPBA). In this reaction, a selenoxide intermediate was obtained and this unpurified crude oil was mixed with acetic anhydride to introduce an acetyl group. After purification, the selenosugar **2c** was isolated in 70% yield. In this case, the β anomer was isolated, which the Pummerer rearrangement can explain.^[43] Due to the steric hindrance, the introduction of the acetyl group is favored by the face opposite to the isopropylidene group. This result is analogous to that reported by Pinto et al. using the Pummerer reaction in the stereoselective synthesis of 4'-selenonucleosides.^[44] Finally, the TBDPS protecting group was removed using a solution of TBAF in THF. Derivatives **2d** and **2e** were obtained in ~70% yields.



Scheme 2. Synthesis of selenium-containing compounds.

From the analysis of the ¹H NMR spectra, the stereochemistry of each of the stereocentres generated in the preparation of **2d** and **2e** was determined. The selenium atom distorts the rings of the monosaccharides. This distortion could explain the difference between $J_{3,4\text{-trans}}$ in the O-containing furanose cycle^[45] and the Se-containing furanose cycle.^[42] Theoretical DFT calculation of dihedral angles was also performed to better understand the relationship between J and φ . Figure 2 shows **2d**, **2e**, and **2e**(α) optimized minimum energy structures. The alpha isomer was not obtained, it was included in the theoretical calculation for comparison. The coupling constants were calculated at

B3LYP/TZVP^[46] level of theory in good agreement with the experimental values.^[47] The calculations predict an φ value close to 90° for the protons H1a-H2 and H3-H4 in compound **2d**, corresponding to low values of J (see Table 1). The maximum J was observed for H2 and H3 with $\varphi \approx 0^\circ$ and slightly decreased for H1b with $J=5.2$ Hz. In general, the system's geometry changes slightly with the introduction of the acetyl group. The value of J_{H1a-H2} obtained for **2e** corresponds to the estimated φ , being close to 90° it would correspond to a low J . Therefore, if acetylation had occurred on the alpha side, an intermediate J value would be expected.

RESEARCH ARTICLE

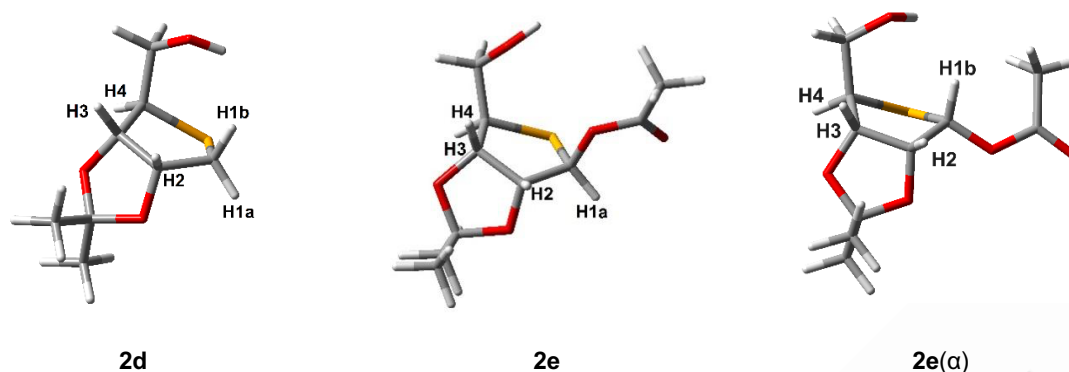
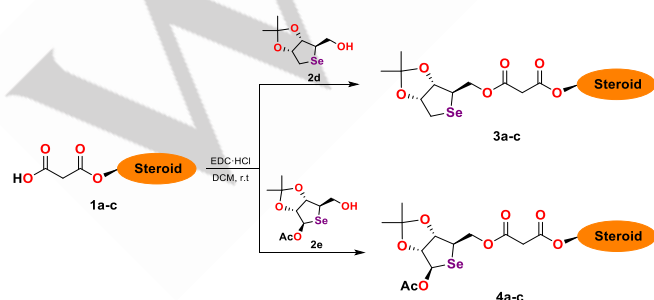


Figure 2. Optimized minimum energy structures of **2d**, **2e**, and **2e(α)** at DFT-B3LYP-D3(BJ)/6-311G(2d,p) level.

Table 1. Experimental and theoretical *J* values calculated at B3LYP/TZVP level of theory and dihedral angles (φ) (H-C-C-H) for the selenosugars **2d**, **2e**, and **2e(α)**.

Compound	Dihedral angle calculated (φ)				Experimental/Calculated <i>J</i>			
	H1a-H2	H1b-H2	H2-H3	H3-H4	H1a-H2	H1b-H2	H2-H3	H3-H4
2d	90.2	32.5	3.3	90.8	2.1/0.9	5.2/5.3	5.5/6.3	1.4/0.8
2e	85.2	-	23.4	121.2	<1/1.4	-	5.4/5.4	<1/2.3
2e (α)	-	46.3	11.2	102.9	-	-4.4	-5.9	-0.8

The selenosugars **2d** and **2e** were linked to the steroidal acids **1** by esterification reaction to obtain new selenosugar-steroid conjugates. In this case, we used EDC as carbodiimide in anhydrous dichloromethane at room temperature, see Scheme 3. The new six selenosugar-steroid conjugates were obtained as white solids after purification by column chromatography in yields between 72–85%. These derivatives represent the first report of the conjugation of steroids to selenosugars. This method proved to be efficient for conjugating steroids to both monosaccharides and selenosugars, with slightly higher yields for the latter.^[35] The lowest yields were obtained for the estradiol derivatives, which could be related to the potential interference of the phenolic function in the reaction. As expected, the presence of the acetyl group did not interfere with the conjugation results.



Scheme 3. Conjugation reaction between steroid malonates (**1**) and selenosugars (**2**). Steroid, a: cholesterol, b: diosgenine, c: estradiol.

The novel conjugates were fully characterized by NMR spectroscopic techniques (see Supporting Information). ¹H NMR shows the signals corresponding to the malonate linker, the

steroid moieties, and the selenosugar fragment. In particular, the methylene protons of the malonate fragment appear as a singlet around ~ 3.40 ppm. Some representative protons of cholesterol and diosgenin such as H3 and H6 are found at ~ 4.66 and ~ 5.37 ppm, respectively. In the case of estradiol, the protons of the aromatic ring appear at 7.13–6.56 ppm. On the other hand, the methylene protons (H5) of the selenosugar fragment are deshielded at ~ 4.34 and ~ 4.19 ppm for conjugates **3** and at ~ 4.39 and ~ 4.24 ppm for conjugates **4** in comparison to the same protons in compounds **2d** (4.00 and 3.91 ppm) and **2e** (3.77 ppm). The ¹³C NMR spectrum shows signals at ~ 166 and ~ 165 ppm corresponding to the two carbonyl groups of the malonate moiety. The assignment of all carbon and proton signals was carried out by the combination of HSQC and HMBC experiments, see the spectra in the Supporting Information.

It was interesting to perform theoretical calculations to analyze the structure of the synthesized compounds and their properties in more detail. Previous work on similar molecular systems has demonstrated the benefits of combining semi-empirical methods and DFT for the conformational study and determination of molecular and geometric properties of new conjugates.^[48] This strategy allows the reduction of computational effort and exhaustively the potential energy surface. A series of structures with the O=C...C=O dihedral angle rotation were pre-calculated using a semiempirical PM6 method.^[49] After the pre-optimization, structures of minima energy were submitted to a full optimization with the B3LYP^[50] hybrid functional together with D3(BJ) correction and the 6-311G (2d,p) basis set, affording the lowest energy conformations presented in Figure 3.

RESEARCH ARTICLE

Malonate group interacts actively forming hydrogen bonding. Calculations predicted a tendency to a relative *s*-trans conformation of the carbonyl groups of the malonate unit, more significantly when acetyl groups are presented. The $O=C\cdots C=O$ dihedral angle has a value from around -100.3° to -160.2° for all cases. The results are in agreement with those previously reported by our research group.^[34] Interaction of H3 of the corresponding ring A of the steroid moieties (cholesterol and diosgenin) with the malonate carbonyl was found. The carbonyl's *s*-trans conformation in the malonate moiety allows the formation of a weak interaction $C=O\cdots H-C3$ with the hydrogen of the closest ring, being achieved through a twisted boat conformation of ring A.

The Meldrum's acid moiety also seems to be a hydrogen bond acceptor for the methylene group of the selenosugar moiety. In diosgenin moiety, other interaction can be calculated between the oxygen atom and the H12 from ring D, in twisted boat conformation with values between 2.35 - 2.45 Å. The results show that the relative orientation of the malonate carbonyls in structures without the acetyl group is synclinal, whereas, for the acetyl group an antiperiplanar disposition was observed, with dihedral $O=C\cdots C=O$ angles reported in Figure 3. In all cases, the presence of hydrogen bonds has a major role in the final geometry of these molecules.

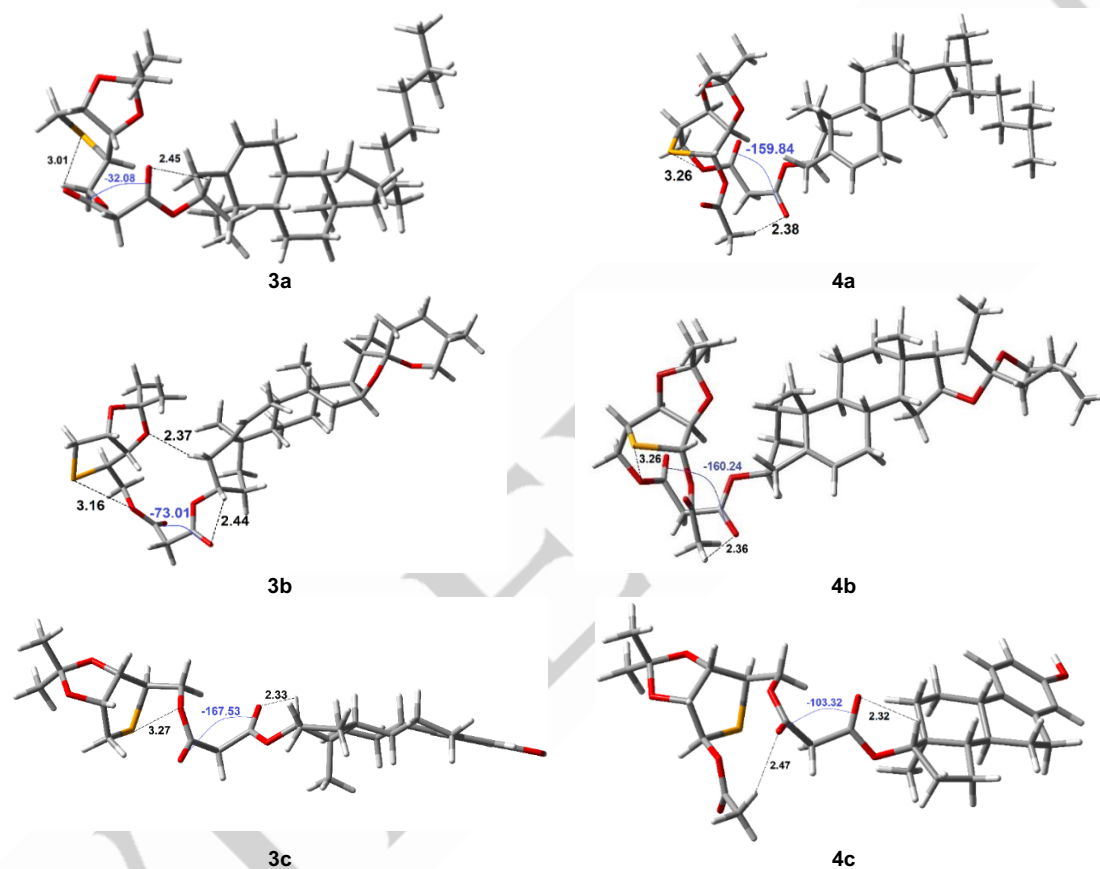


Figure 3. Optimized minimal energy structures of steroid-selenosugar conjugates at the DFT - B3LYP-D3(BJ)/6-311G(2d,p) level.

The results of DFT calculations have shown $CH\cdots Se$ weak interaction of around 3 Å as reported in crystal structures.^[51] Spectroscopic and crystal structure investigations also confirmed the presence and significance of selenium interactions within biomolecular systems, the crystal packing, and the synthesis of chiral selenones. They demonstrated that based on statistical results, selenium tends to build interactions of the $CH\cdots Se$ type. Another interaction $Se\cdots O$ around 3.23 and 3.27 Å is reported.^[52] HOMO and LUMO are fundamental quantum chemical parameters to determine the reactivity of the molecules. Furthermore, HOMO-LUMO energy difference is a measure of the intramolecular charge transfer and has been used to correlate biological assay with electrostatic results.^[53] The energies of the HOMO and LUMO of the studied compounds and their isodensity

surface plots are represented in Figures S58 and S59 in the Supporting Information. From the depiction of molecular orbitals, it can be observed that the HOMO orbitals consist mainly of the nonbonding electron pairs on the selenium atom. In the case of **3c** and **4c** compounds, the HOMO is an antibonding combination between the hydroxyl oxygen and π -orbitals of the benzene ring. The electrons in these orbitals are the most reactive against electrophilic reagents because the lowest ionization energy is obtained. The electron density of the LUMO is located mainly in the malonate group when the main LUMO's character is the π -antibonding orbital of the carbonyl group. LUMO's energy is closely related to reactivity against nucleophile attack, when the acetyl group is included in the molecules, the electron affinity

RESEARCH ARTICLE

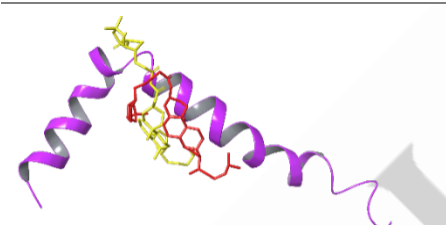
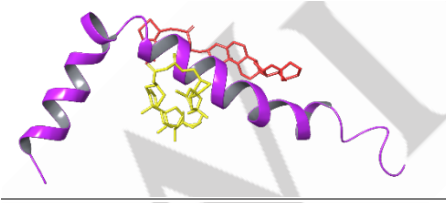
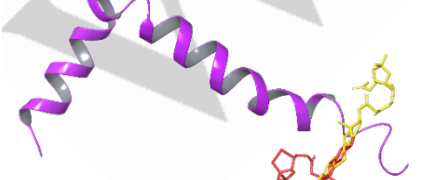
increases. A bandgap from 5.21 eV to 5.37 eV has been predicted for these conjugates.

It has been described in the literature that the LUMO energy can be related to biological outcomes, observing that the most stabilized LUMO orbitals have the best biological response.^[53a] In this case, the most stable LUMO of the non-acetylated conjugates correspond to those derived from cholesterol (**3a**, -0.72 eV) and estradiol (**3c**, -0.74 eV), whereas the energy values of the acetylated conjugates (**4a-c**) are similar.

Molecular docking is a useful tool that can be used in the early stages of research and can be an excellent starting point for predicting potential inhibitors of a particular target. It has been studied that the amino acid Lys-16 plays an essential function in the formation of A β oligomers, due to its proximity to the hydrophobic nucleus region between Leu-17 and Ala-21.^[54] In this sense, the interaction of **3** and **4** conjugates with the A β was studied by molecular docking using AutoDock Tools and AutoDock 4.2.5.1.^[55] The protein target employed was the A β (PDB ID: 1IYT)^[56] and the minimal energy conformations of the selenosugar-steroid derivatives obtained by DFT calculations were used as ligands, see Computational details in the Experimental Section.

According to the calculations, all the conjugates showed an affinity for the receptor, with average values between 5 and 7 kcal/mol (see Table 2).

Table 2. Low-energy binding conformations of **3** and **4** conjugates bound to A β peptide generated by molecular docking.

Superimposed conformation	Affinity ^a
	$E_{3a} = -6.1$ kcal/mol $E_{4a} = -4.9$ kcal/mol
	$E_{3b} = -6.0$ kcal/mol $E_{4b} = -7.5$ kcal/mol
	$E_{3c} = -6.1$ kcal/mol $E_{4c} = -6.1$ kcal/mol

The A β peptide is shown in the cartoon model and the ligands are represented in sticks, **3** in red and **4** in yellow. ^a Affinity expressed in kcal/mol.

From an energetic point of view, no major differences were observed in ligand affinities associated with the structures of different steroids. For the conjugates of cholesterol (**3a** and **4a**) and estradiol (**3c** and **4c**), it will be observed that the interaction

with the peptide occurs mainly through the steroidal skeleton based on hydrophobic and π - π stacking interactions. The introduction of an *O*-acetyl group in the diosgenin conjugates (**3b** and **4c**) caused a variation in the interaction zone of the conjugate, although the energy was slightly increased, the *O*-acetyl group did not present interactions with the peptide residues. The conjugates of cholesterol and diosgenin present interactions (See Table S2 in the Supporting information) mainly with the residues included in the His-13 and Lys-29 region, the main region described in forming molecular aggregates.^[17] The presence of an aromatic ring in the skeleton of estradiol makes its derivatives have an affinity for the Glu-3 and His-14 region favored by the π - π stacking interaction with the Tyr-10.

The results of the interaction of the A β with the conjugates **3** and **4** and the possibility of its functionalization due to the presence of a malonic linker, suggested evaluating the influence of a C₆₀ unit linked to the conjugates. The C₆₀ could increase the interaction zones with the aromatic and hydrophilic residues of the protein, in addition to the contribution it makes due to its known biological properties.^[13] Figure 4 shows the designed structures of selenosugar-steroid-[60]fullerene for the theoretical evaluation.

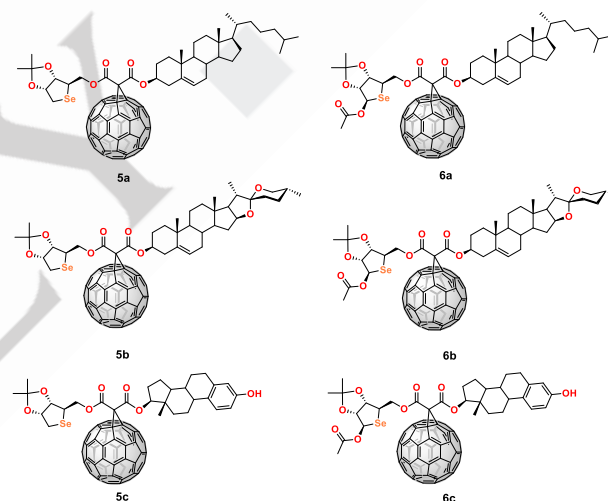


Figure 4. Designed structures of fullerene derivatives for molecular docking calculations.

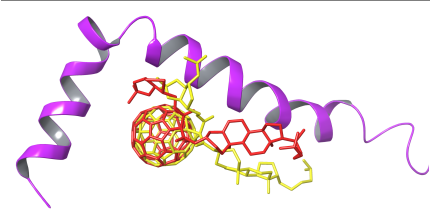
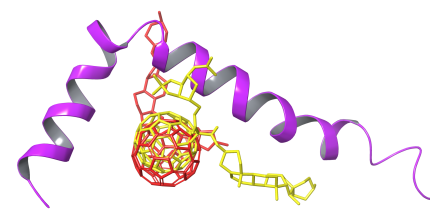
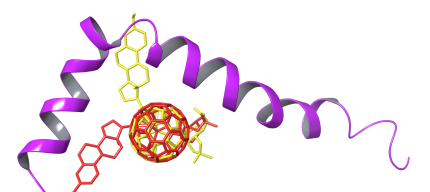
The molecular docking calculations were carried out under the same conditions as for the selenosugar-steroid conjugates, for more information see the Experimental Section. Representative superimposed complexes of the fullerene derivatives and affinity values for the A β are shown in Table 3.

It can be inferred that the presence of C₆₀ slightly increases the affinity concerning the corresponding steroid-selenoconjugates. In all complexes obtained, the fullerene core anchors in the hydrophobic cavity of the A β peptide, allowing the moieties to interact with neighboring residues. Similar studies carried out with methanofullerenes reveal the importance of π - π stacking and hydrophobic interactions of fullerene core, especially in the hydrophobic pocket.^[57] The fullerene core interacts with the peptide in all cases with Phe-20 and Leu-34. All monoadducts presented interactions with Val-24 except **6b** and only **5a** with Lys-28. These two residues have been reported as key in the interaction of free cholesterol with the A β .^[21] Cholesterol derivatives, despite having slightly lower affinity values,

RESEARCH ARTICLE

conjugates **5a** and **6a** present similar binding modes with residues reported as key for anti-aggregation, see Figure 5.

Table 3. Superimposed conformations of **5**-A β and **6**-A β generated by molecular docking. The A β is shown in the cartoon model and the ligands are represented in sticks, **5** in red and **6** in yellow.

Superimposed conformation	Affinity ^a
	$E_{5a} = -8.5$ $E_{6a} = -8.8$
	$E_{5b} = -9.0$ $E_{6b} = -9.3$
	$E_{5c} = -9.2$ $E_{6c} = -8.9$

The A β peptide is shown in the cartoon model and the ligands are represented in sticks, **5** in red and **6** in yellow. ^a Affinity expressed in kcal/mol.

In the case of diosgenin, only acetylated derivative (**6b**) presented a binding mode similar to that of cholesterol. Estradiol monoadducts have binding modes with completely different residues from those of cholesterol found in the C-terminal region. The residue Leu-17 interacted in all the complexes with the steroidal fragment and the selenosugar. At the same time, Leu-

16 formed hydrogen bonds with the selenosugar moiety (**5b** and **5c**) and cation- π with the fullerene surface (**6c**). The other interactions are represented in Supporting Information, see Tables S3.

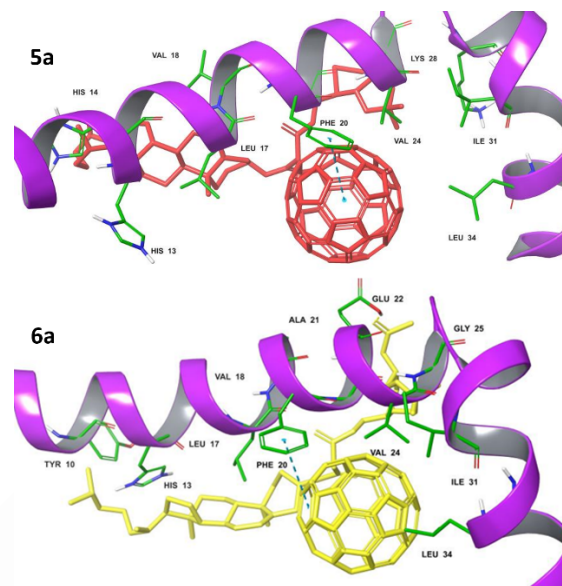
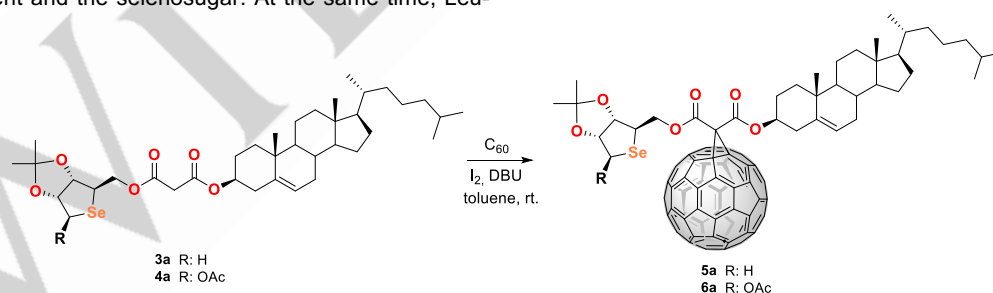


Figure 5. Designed structures of fullerene derivatives for molecular docking calculations.

Considering the preliminary results of the interaction of series **5** and **6** derivatives with the A β and the similarity in the reported specific binding modes of free cholesterol,^[21] it was interesting to obtain derivatives **5a** and **6a**. The covalent attachment of the obtained malonates **3a** and **4a** to the C₆₀ was carried out by cyclopropanation under Bingel–Hirsch conditions.^[58] The cyclopropanation reaction was carried out at room temperature by mixing the [60]fullerene dissolved in anhydrous toluene with the malonates **3a** and **4a**, molecular iodine, and DBU (see Scheme 4).



Scheme 4. Synthesis of cholesterol monoadducts **5a** and **6a**.

After two hours the reaction was completed and the reaction mixture was purified by column chromatography. The excess unreacted C₆₀ was eluted with carbon disulfide and the monoadducts with chloroform as eluent. The monoadducts were obtained as brown solids, with 50% (**5a**) and 77% (**6a**) yields. The new two monoadducts are soluble in common organic solvents such as chloroform, dichloromethane, dimethylsulfoxide (2 mg/mL), and also water (2 mg/mL after efficient sonication).

The structural elucidation of the fullerene derivatives was carried out by combining different spectroscopic techniques (see Experimental Section and Supporting Information). The UV/Vis spectra of compounds **5a** and **6a** supported the formation of [6,6]-closed fullerene adducts, because both spectra show the typical band centered at 428 nm. This band caused by π - π and n - π electronic transitions differentiates the monoadducts from non-functionalized C₆₀.^[59] Superimposed spectra of derivatives **5a**, **6a**,

RESEARCH ARTICLE

and C₆₀ in toluene are shown in Figure S55 of the Supporting Information.

¹H NMR Spectroscopy confirmed the suggested structures for the hybrid derivatives **5a** and **6a** because in both spectra the absence of the singlet at $\delta = 3.40$ ppm was observed. It was detected that signals of protons near the fullerene surface are slightly unshielded when functionalization occurs. For example, the protons H6 and H3 have signals of 5.51 and ~ 4.66 ppm, respectively, while in the precursor malonates (**3a** and **4a**) they present these signals with a difference of more than 0.7 ppm. During the functionalization, [60]fullerene loses its symmetry, so in the carbon spectra, many signals are observed in the range of 145 to 141 ppm, confirming the carbon sphere's introduction. Furthermore, malonate carbonyl signals are identified at ~ 163 and ~ 162 , shielded at almost 3 ppm from conjugates **3** and **4** before coupling to fullerene. Finally, the mass spectroscopy confirms the structures proposed. The MALDI spectrum of **5a** shows a peak at $m/z = 1409.9729$ (calculated for C₉₈H₅₈O₆Se 1410.3398) corresponding to M⁺. Instead, the corresponding molecular peak of **6a** was not observed, but the $m/z = 1453.2799$ (calculated for C₉₉H₅₇O₈Se 1453.3218) corresponding to the fragmentation with the lowest mass loss of 15 u was identified. Considering the structural difference with **5a**, this behavior may be related to the presence of an acetyl group in the selenosugar fragment. (see Figure S56 and S57 in the Supporting Information) From the theoretical point of view, the optimized minimal energy structures of **5a** and **6a** were obtained at the DFT- B3LYP-D3 (BJ)/6-311G(2d,p) level (Figure 6). Here again, malonate groups interact forming intramolecular hydrogen bonding. A tendency to the *s-trans* conformation of the carbonyl groups is presented. The O=C...C=O dihedral angle has a value from around -73° to -97° . Interaction of H3 of the corresponding ring A of the cholesterol moieties was also found. To get a better understanding of the geometrical features, a Non-Covalent Interactions (NCI) analysis was performed, see Figure 7.

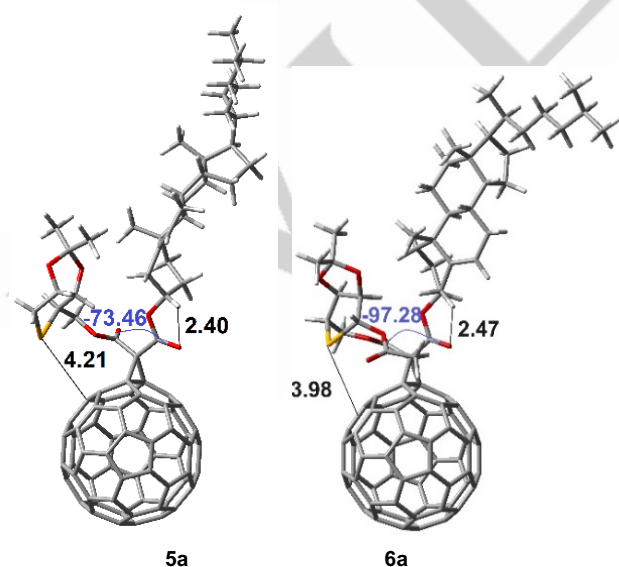


Figure 6. Optimized minimal energy structures of fullerene derivatives at the DFT- B3LYP-D3 (BJ) / 6-311G(2d,p) level.

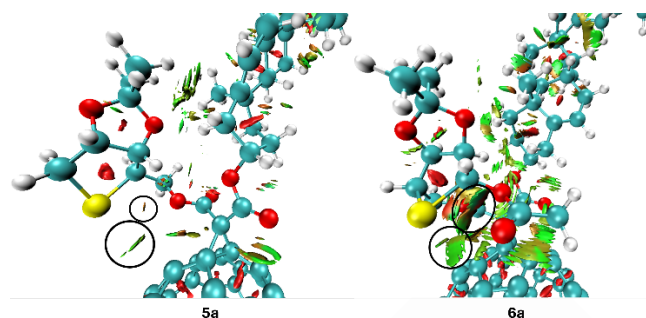


Figure 7. NCI analysis of hybrids **5a** and **6a**. Isosurfaces represent the regions of interactions where green represents attractive interactions and red strong repulsive interactions. Interactions of selenium atoms are highlighted in black.

This approach is based on the reduced density gradient (RDG) and is used both to evaluate the nature of weak interactions and to characterize intramolecular or intermolecular interactions by isolating these interactions as the regions with a low reduced density gradient at low-density values.^[60] Results revealed weak interactions through simple color codes. Green regions represent the van der Waals interactions, weak intermolecular interactions with lower electron densities. Several weak intramolecular interactions are obtained specifically between the hydrogens and the carbonyl groups, Se... π (C₆₀), Se...O. There are reports from the literature of this kind of interaction playing an important role in the stability of protein structures, like DNA structures.^[61] Other research groups reported the nature of intermolecular Se... π interaction through theoretical study.^[62]

The energies of the HOMO and LUMO of the fullerene derivatives and their isodensity surface is represented in Figure S60 of the Supporting Information. In both cases, the HOMO and LUMO orbitals are extended over the fullerene core. The presence of fullerene considerably decreases the LUMO energy for both hybrids by more than 2.5 eV compared to conjugates **3a** and **4a** without fullerene (see Table S1 of the Supporting Information). Therefore, the presence of the fullerene cage could increase the biological activity of the compounds in correspondence with the decrease in LUMO energy. Low LUMO energies give rise to the best ligand-protein interactions.^[54a] Moreover, to evaluate the intramolecular electrostatic interactions in hybrids **5a** and **6a**, the electron density surrounding each molecular hybrid was calculated at the same level of theory. The resulting electrostatic molecular potential map is shown in Figure 8. The covalent attachment of the steroid and selenosugar moieties to the fullerene cage induced a change in the electrostatic potential distribution due to weak charge separation. In this regard, the negative potential, represented by red color, was mainly associated with the selenium atom and the oxygen atoms belonging to carbonyl functions, whereas positive regions marked by blue color were located at some part of the steroid backbone. Most of the uncharged green zones are distributed throughout both molecular conjugates, which predicts an enhancement of the hydrophobic character of both compounds, making them more soluble in non-polar solvents.

RESEARCH ARTICLE

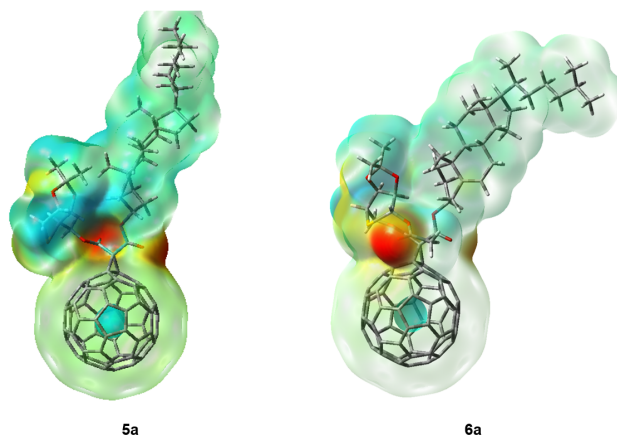


Figure 8. Electrostatic molecular potential maps for the most stable fullerene derivatives **5a** and **6a** conformations.

In addition, such electrostatic distribution could be beneficial to increase the lipophilicity of compounds **5a** and **6a**, as indicated by the calculated $\log P^{[63]}$ values of 17.76 and 17.17, respectively. Nevertheless, despite the small charge separation, dipole moments of 5.98 D (**5a**) and 5.74 D (**6a**) were predicted. Moreover, the topological polar surface area (TPSA)^[64] was calculated to estimate the interaction with biological membranes. In this case, the TPSA for **5a** (71.06 Å²) and **6a** (97.36 Å²) are in correspondence with optimal values (<120 Å²) based on comparison with approved drugs.^[65] Therefore, considering these results, it is expected that these hybrid molecules could penetrate lipid membranes and the BBB, which would be paramount for prospective biological applications.^[66] These findings agree with the results reported for similar compounds.^[67] The new hybrid compounds, which contain fullerene, steroids, and selenosugar units in the same molecule, can be considered promising derivatives, whose potential in biomedical applications will be explored.

Conclusion

In the search for compounds that inhibit the oligomerization of A β , in this work, we report the synthesis of new hybrid compounds based on fullerene decorated with fragments of biological interest. The reaction was carried out using Bingel's cyclopropanation method, which involves the formation of a malonate containing steroid and selenosugar fragments.

The required starting malonates were prepared in a multistep synthetic procedure in which the steroidal acids, synthesized by treatment of three different sterols – cholesterol, diosgenin, and estradiol– with Meldrum acid, were connected to two selenosugar units, prepared in a straightforward manner from the D-riboniclactone. This procedure led to the formation of six new selenosugar-steroid conjugates. A thorough spectroscopic study has allowed the chemical structures of the new compounds to be unambiguously determined. Theoretical calculations at the DFT-B3LYP-D3(BJ)/6-311G(2d,p) level show that weak interactions play an important role in the geometry of the studied molecules, and predict the CH \cdots Se and Se \cdots O interactions (around 3 Å). In

the case of the hybrid-fullerene compounds noncovalent interaction Se \cdots π (C₆₀) was obtained at around 4 Å. Computational modeling showed that malonate groups interact forming intramolecular weak interactions and a tendency to the s-trans conformation of the carbonyl groups are presented. For fullerene derivatives, the smallest HOMO-LUMO gap energies were obtained, which induces the highest influence on intramolecular charge transfer and bioactivity. Molecular docking investigations predicted the application of these compounds as potential inhibitors of the A β oligomerization. These are promising results to further explore the biological applications of these structures.

Experimental Section

Computational details

All computations were performed with the Gaussian 09 suite of programs^[68] and molecules were built with Avogadro.^[69] We first generated a grid by rotating the dihedral O=C \cdots C=O malonate, rotations were made every 30°. These geometries were fully relaxed using the PM6 semiempirical Hamiltonian as a satisfactory starting point.^[70] Afterward, redundant structures are discarded according to energy degeneracies and RMSD similarities. The remaining structures were fully relaxed with the B3LYP^[50] density functional adding the D3(BJ) Grimme's dispersion correction and the 6-311G(2d,p) Pople's basis set.^[71] Stationary points were characterized by harmonic vibrational analysis to ensure that they represent minima on the potential energy surface. Then the most stable conformers were selected for the analysis. To check the confidence of the obtained results, optimizations of some structures were also repeated with the wB97XD/6-311G(2d,p) method,^[72] and nearly identical geometries were obtained. The frontier orbitals HOMO/LUMO were visualized directly from the optimized structure and this conformation was used for the calculation of the electrostatic molecular potential map using the same DFT level and Gaussview 6.0 software.^[73] The reduced density gradient (RDG) analysis was performed by using the non-covalent interactions (NCI) theory and using the Multiwfn program (Multifunctional Wavefunction Analyzer)^[74] for realizing electronic wavefunction analysis using suggested default values. For the analysis, the results were visualized with the VMD (Visual Molecular Dynamics) software.^[75]

Molecular Docking

Ligand/Protein Preparation. The ligand-optimized structures were obtained from the lowest energy conformations previously calculated. The structure of the A β (PDB ID: 1IYT)^[57] was used as the model from Protein Data Bank (PDB) (<http://rcsb.org>). The protein was processed by removing water and adding polar hydrogen atoms. Default rotatable bonds were retained, except for the fullerene that was set to un-rotatable. The Gasteiger model was used for the calculations of the partial charges of the ligands. The protein and ligand structures were saved in PDBQT format with AutoDock Tools.^[76] The center of the simulation box was centered (-1.00, 0.00, 1.00) with size of 60 × 60 × 70 Å³.

RESEARCH ARTICLE

Simulation and Analysis of Target-Ligand Complexes: Molecular docking was performed using AutoDock 4.2.5.1.^[56] Docking parameters were set to default. Ten independent runs were performed in each case, and the two best-docked conformations of each run were analyzed, according to the affinity calculated with the scoring function. The total docked conformations were grouped based on the Root Mean Square Deviation (RMSD) of the different bound poses. The RMSD difference between conformations of the same cluster was set to less than 2 Å. Every cluster's binding free energy (kcal/mol) was calculated as the mean binding free energy (MBFE) of all the conformations present in the same cluster. Molecular interactions between the ligand and the binding site residues of the protein were analyzed using Discovery Studio.

Synthesis of C₆₀ monoadducts

In a 250 mL round flask, [60]fullerene (64 mg, 0.09 mmol) was dissolved in dry toluene (130 mL) in a nitrogen atmosphere. Then the steroid malonate **3a** (41 mg, 0.06 mmol) or **4a** (50 mg, 0.06 mmol), and molecular iodine (23 mg, 0.09 mmol) were added. The system was cooled in an ice bath, the DBU (0.17 mL, 1.13 mmol) was added dropwise and the reaction was stirred for 2 hours. Then water (50 mL) was added and the mixture was partitioned between water and toluene. The organic phase was washed with sodium thiosulfate, brine, separated, and dried over anhydrous Na₂SO₄. The solvent was removed under reduced pressure. The product was purified by column chromatography, using carbon disulfide to elute the C₆₀ that remained unreacted and chloroform for the monoadduct.

Supporting Information

The supporting information contains descriptions of full materials and instruments used, details of synthetic procedures, theoretical calculation details, and analytic methods employed to characterize all new organic molecules reported. The ¹H, ¹³C, HSQC, HBMC, and COSY NMR spectra of the synthesized compounds and for fullerenes derivatives, UV and mass spectra are also included.

Acknowledgements

The authors thank the financial support from the PNCB of MES, Cuba (PN223LH010-019) and *Organizzazione Internazionale Italo-Latina Americana* (IILA) and the ERASMUS + KA 171 program for international mobility financing. Moreover, we acknowledge ETI-BioCubaFarma for providing the resources used in this report. Y. Pérez-Badell thanks Y. M. Álvarez-Ginarte and R. Suardiaz for their support in obtaining the TPSA parameter and coupling constants respectively.

Keywords: β-amyloid • fullerene • organoselenium compound • steroids • theoretical calculations

[1] M. Stefani, C. M. Dobson, *J. Mol. Med.* **2003**, *81*, 678–699.

[2] F. Chiti, C. M. Dobson, *Annu. Rev. Biochem.* **2006**, *75*, 333–366.

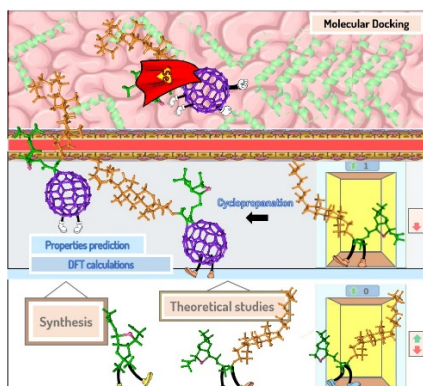
- [3] S. N. Iaroshkin, S. A. Klyushnikov, V. A. Vigont, Y. A. Seliverstov, E. V. Kaznacheyeva, *Biochemistry*, **2018**, *83*, 1030–1039.
- [4] L. V. Kalia, A. E. Lang, *Lancet*, **2015**, *386*, 896–912.
- [5] V. M. Lee, M. Goedert, J. Q. Trojanowski, *Annu. Rev. Neurosci.* **2001**, *24*, 1121–1159.
- [6] M. P. Murphy, H. LeVine, *J. Alzheimer's Dis.* **2010**, *19*, 311–323.
- [7] B. C. Karisetty, A. Bhatnagar, E. M. Armour, M. Beaver, H. Zhang, F. Elefant, *Front. Mol. Neurosci.* **2020**, *13*, 577622.
- [8] D. Schenk, G. S. Basi¹, M. N. Pangalos, *Cold Spring Harb. Perspect. Med.* **2012**, *2*, a006387.
- [9] D. Paris, N. Patel, A. Quadros, M. Linan, P. Bakshi, G. Ait-Ghezala, M. Mullan, *Neurosci. Lett.* **2007**, *415*, 11–16.
- [10] N. L. Sikanyika, H. C. Parkington, A. I. Smith, Sanjaya Kuruppu, *Neurochem. Res.* **2019**, *44*, 1289–1296.
- [11] F. Moraca, I. Vespoli, D. Mastroianni, V. Piscopo, R. Gaglione, A. Arciello, M. De Nisco, S. Pacifico, B. Catalanotti, S. Pedatella, *RSC Med. Chem.* **2024**, *15*, 2286–2299.
- [12] M. Stefani and C. M. Dobson, *J. Mol. Med.* **2003**, *81*, 678–699.
- [13] a) I. Y. Podolski, Z. A. Podlubnaya, E. A. Kosenko, E. A. Mugantseva, E. G. Makarova, L. G. Marsagishvili, M. D. Shpagina, Y. G. Kaminsky, G. V. Andrievsky, V. K. Klochkov, *J. Nanosci. Nanotechnol.* **2007**, *7*, 1479–1485; b) S. Ye, T. Zhou, D. Pan, Y. Lai, P. Yang, M. Chen, Y. Wang, Z. Hou, L. Ren, Y. Jiang, *J. Biomed. Nanotechnol.* **2016**, *12*, 1820–1833; c) F. Y. Hsieh, A. V. Zhilenkov, I. I. Voronov, E. A. Khakina, D. V. Mischenko, P. A. Troshin, S. Hsu, *ACS Appl. Mat. Interfaces*, **2017**, *9*, 11482–11492. d) Z. Liu, Y. Zou, Q. Zhang, P. Chen, Y. Liu, Z. Qian, *Int. J. Mol. Sci.* **2019**, *20*, 2048.
- [14] B. Yang, Y. Chen, J. Shi, *Nanomedicine Chem. Rev.* **2019**, *119*, 4881–4985.
- [15] Y. Ishida, T. Fujii, K. Oka, D. Takahashi, K. Toshima, *Chem. Asian J.* **2011**, *6*, 2312–2315.
- [16] A. G. Bobylev, O. Kraevay, L. G. Bobylev, E. A. Khakina, R. S. Fadeev, A. V. Zhilenkov, D. V. Mishchenko, N. V. Penkov, I. Y. Teplov, E. I. Yakupova, I. M. Vikhlyantsev, P. A. Troshin, *Colloids Surf. B Biointerfaces*, **2019**, *183*, 110426.
- [17] L. Xie, Y. Luo, L. Lin, W. Xi, X. Yang, G. Wei, *Nanoscale*, **2014**, *6*, 9752–9762.
- [18] L. M. Garcia-Segura, J. Balthazart, *Front. Neuroendocrinol.* **2009**, *30*, v–ix.
- [19] S. Veiga, L. M. Garcia-Segura, I. Azcoitia, *Rev. Neurol.* **2004**, *39*, 1043–1051.
- [20] C. J. Pike, J. C. Carroll, A. Barron, E. R. Rosario, *Front. Neuroendocrinol.* **2009**, *30*, 239–258.
- [21] C. Di Scala, H. Chahinian, N. Yahi, N. Garmy, J. Fantini, *Biochemistry* **2014**, *53*, 4489–4502.
- [22] M. Nishio, Y. Umezawa, J. Fantini, M. S. Weiss, P. Chakrabarti, *Phys. Chem. Chem. Phys.* **2014**, *16*, 12648–12683.
- [23] J. Fantini, F. J. Barrantes, *Biochim. Biophys. Acta*, **2009**, *1788*, 2345–2361.
- [24] N. Arispe, M. Doh, *FASEB J.* **2002**, *16*, 1526–1536.
- [25] C. Di Scala, N. Yahi, C. Lelievre, N. Garmy, H. Chahinian, J. Fantini, *ACS Chem. Neurosci.* **2013**, *4*, 509–517.
- [26] X. Yang, C. Tohda, *Sci. Rep.* **2018**, *8*, 11707.
- [27] C. Tohda, Y. A. Lee, Y. I. Goto, Y. I. Nemere, *Sci. Rep.* **2013**, *3*, 3395.
- [28] C. Tohda, T. Urano, M. Umezaki, I. Nemere, T. Kuboyama, *Sci. Rep.* **2012**, *2*, 535.

RESEARCH ARTICLE

- [29] S. Som, J. Antony, S. Dhanabal, S. Ponnusankar, *Metab. Brain Dis.* **2022**, *37*, 359–372.
- [30] C. W. Nogueira, J. B. T. Rocha, *Arch. Toxicol.* **2011**, *85*, 1313–1359.
- [31] A. K. Witt, K. E. Sandoval, *Adv. Pharmacol.* **2014**, *71*, 361–390.
- [32] E. I. El-Desoky, M. Reyad, E. M. Afsah, A. M. Dawidar, *Steroids*, **2016**, *105*, 68–95.
- [33] F. Song, M. Zheng, J. Wang, H. Liu, Z. Lin, B. Liu, Z. Deng, H. Cong, Q. Zhou, X. Qu, *Nat. Synth.* **2023**, *2*, 729–739.
- [34] a) L. Almagro, R. Lemos, K. Makowski, H. Rodríguez, O. Ortiz, W. Cáceres, M. Á. Herranz, D. Molero, R. Martínez, M. Suárez, N. Martín, *Eur. J. Org. Chem.* **2020**, *2020*, 5926–5937; b) M. Suarez, K. Makowski, R. Lemos, L. Almagro, M. Á. Herranz, D. Molero, H. Rodriguez, N. F. Albericio, Y. Murata, N. Martín, *ChemPlusChem*. **2021**, *86*, 972–981; c) R. Lemos, F. Ortiz, L. Almagro, K. Makowski, N. Martín, F. Albericio, M. Suarez, H. Rodriguez, *Surf. Interface Anal.* **2022**, *10*, 1041–1051.
- [35] R. Lemos, K. Makowski, L. Almagro, B. Tolón, H. Rodríguez, M. Á. Herranz, D. Molero, N. Martín, M. Suárez, *Eur. J. Org. Chem.* **2023**, *26*, e202201301.
- [36] a) F. F. Irsafli, L. Mahdavian, A. Marjani, *Comput. Theor. Chem.* **2023**, *1230*, 114376; b) M. H Abdellatif, A. H. Abdel-Rahman, M. M. H. Arief, S. M. Mounier, A. Ali, M. A. Hussien, R. M. Okasha, T. H. Afifi, M. Hagar, *Front. Chem.* **2021**, *9*, 672503.
- [37] D. Wu, D. G. Truhlar, *J. Chem. Theory Comput.* **2021**, *17*, 3967–3973.
- [38] C. Bingel, *Chem. Ber.* **1996**, *26*, 1957–1959.
- [39] G. Cimmino, M. De Nisco, S. Piccolella, C. Gravina, S. Pedetella, S. Pacifico, *Antioxidants*, **2024**, *13*, 744.
- [40] a) M. Milen, T. Szabó, *Chem. Heterocycl. Comp.* **2019**, *55*, 936–938; b) U. Alehagen, T. B. Opstad, J. Alexander, A. Larsson, J. Aaseth, *Biomolecules*, **2021**, *11*, 1478; c) W. Hou, H. Xu, *J. Med. Chem.* **2022**, *65*, 4436–4456.
- [41] a) S. J. Ahn, M. Koketsu, H. Ishihara, S. M. Lee, S. K. Ha, K. H. Lee, T. H. Kang, S. Y. Kim, *Chem. Pharm. Bull.* **2006**, *54*, 281–286; b) F. Zhang, X. Li, Y. Wei, *Biomolecules*, **2023**, *13*, 799.
- [42] L. Serpico, M. De Nisco, F. Cermola, M. Manfra, S. Pedatella, *Molecules*, **2021**, *26*, 2541.
- [43] L. Smith, S. C. Coote, H. F. Sneddon, D. J. Procter, *Angew. Chem. Int. Ed.* **2010**, *49*, 5832–5844.
- [44] K. Jayakanthan, B. D. Johnston, B. M. Pinto, *Carbohydr. Res.* **2008**, *343*, 1790–1800.
- [45] L. Benhamou, R. W. Foster, D. P. Ward, K. Wheelhouse, L. Sloan, C. J. Tame, D-K Bučar, G. J. Lye, H. C. Hailes, T. D. Sheppard, *Green Chem.* **2019**, *21*, 2035–2042.
- [46] R. H. Contreras, R. Suardiaz, C. Pérez, R. Crespo-Otero, J. San Fabián, J. M. García de la Vega, *Chem. Theory Comput.* **2008**, *4*, 1494–1500.
- [47] E. R. Johnson, S. Keinan, P. Mori-Sánchez, J. Contreras-García, A. J. Cohen, W. Yang, *J. Am. Chem. Soc.* **2010**, *132*, 6498–6506.
- [48] M. Suárez, K. Makowski, R. Lemos, L. Almagro, H. Rodríguez, M. Á. Herranz, D. Molero, O. Ortiz, E. Maroto, F. Albericio, Y. Murata, N. Martín, *ChemPlusChem*, **2021**, *86*, 972–981.
- [49] J. J. P. Stewart, *J. Mol. Model.* **2007**, *13*, 1173–1213.
- [50] A. D. Becke, *J. Chem. Phys.* **1993**, *98*, 5648–5652.
- [51] M. Iwaoka, S. Tomoda, *J. Am. Chem. Soc.* **1994**, *116*, 4463–4464.
- [52] M. Iwaoka, H. Komatsu, T. Katsuda, S. Tomoda, *J. Am. Chem. Soc.* **2004**, *126*, 5309–5317.
- [53] a) S. Kumar, V. Saini, I. K. Maurya, J. Sindhu, M. Kumari, R. Kataria, V. Kumar, *PLoS One*, **2018**, *13*, e0196016; b) Y. N. Mabkhot, F. D. Aldawsari, S. S. Al-Showiman, A. Barakat, S. M. Soliman, M. I. Choudhary, S. Yousuf, M. S. Mubarak, T. B. Hadda, *Chem. Cent. J.* **2015**, *9*, 24.
- [54] K. Brännström, A. Öhman, L. Nilsson, M. Pihl, L. Sandblad, A. Olofsson, *J. Am. Chem. Soc.* **2014**, *136*, 10956–10964.
- [55] G. M. Morris, R. Huey, W. Lindstrom, M. F. Sanner, R. K. Belew, D. S. Goodsell, A. J. Olson, *J. Comput. Chem.* **2009**, *30*, 2785–2791.
- [56] O. Crescenzi, S. Tomaselli, R. Guerrini, S. Salvadori, A. M. D'Ursi, P. A. Temussi, D. Picone, *Eur. J. Biochem.* **2002**, *269*, 5642–5648.
- [57] X. Zhou, W. Xi, Y. Luo, S. Cao, G. Wei, *J. Phys. Chem. B*, **2014**, *118*, 6733–6741.
- [58] X. Camps, A. Hirsch, *J. Chem. Soc.* **1997**, 1595–1596.
- [59] C. Du, J. Xu, Y. Li, W. Xu, D. Zhu, *Chin. Sci. Bull.* **2001**, *46*, 1156–1159.
- [60] E. R. Johnson, S. Keinan, P. Mori-Sánchez, J. Contreras-García, A. J. Cohen, W. Yang, *J. Am. Chem. Soc.* **2010**, *132*, 6498–6506.
- [61] a) G. Duan, V. H. Smith, D. F. Weaver, *Mol. Phys.* **2001**, *99*, 1689–1699; b) I. Hartman, C. A. Raia, R. J. Zauhar, *Biopolymers* **2006**, *83*, 595–613; c) E. S. Arnér, *Exp. Cell Res.* **2010**, *316*, 1296–1303.
- [62] a) M. Saberinasab, S. Salehzadeh, M. Solimannejad, *Comput. Theor. Chem.* **2016**, *1092*, 41–46; b) M. Saberinasab, S. Salehzadeh, Y. Maghsoud, M. Bayat, *Comp. Theor. Chem.* **2016**, *1078*, 9–15.
- [63] P. Gaillard, P. A. Carrupt, B. Testa, A. Boudon, P. Gaillard, P. A. Carrupt, B. Testa, A. Boudon, *J. Comput. Aided Mol. Des.* **1994**, *8*, 83–96.
- [64] A. Mauri, M. Bertola, *Int. J. Mol. Sci.* **2022**, *23*, 12882.
- [65] P. Mohanty, S. Bhatnagar, *Assay Drug Dev. Technol.* **2019**, *17*, 58–67.
- [66] a) J. Wong-Ekkabut, S. Baoukina, W. Triampo, I. M. Tang, D. P. Tieleman, L. Monticelli, *Nat. Nanotechnol.* **2008**, *3*, 363–368; b) C. W. Wong, A. V. Zhilenkov, O. A. Kraevaya, D. W. Mischenko, P. A. Troshin, S. H. Hsu, *J. Med. Chem.* **2019**, *62*, 7111–7125.
- [67] M. S. Bjelakovic, T. J. Kop, R. Baosic, M. Zlatovic, A. Zekic, V. Maslak, D. R. Milic, *Monatsh. Chem.* **2014**, *145*, 1715–1725.
- [68] M. J. Frisch, G. W. T., H. B. Schlegel, G. E. Scuseria, M. A. Robb, J. R. Cheeseman, G. Scalmani, V. Barone, B. Mennucci, G. A. Petersson, H. Nakatsuji, M. Caricato, X. Li, H. P. Hratchian, A. F. Izmaylov, J. Bloino, G. Zheng, J. L. Sonnenberg, M. Hada, M. Ehara, K. Toyota, R. Fukuda, J. Hasegawa, M. Ishida, T. Nakajima, Y. Honda, O. Kitao, H. Nakai, T. Vreven, J. A. Montgomery Jr., J. E. Peralta, F. Ogliaro, M. Bearpark, J. J. Heyd, E. Brothers, K. N. Kudin, V. N. Staroverov, R. Kobayashi, J. Normand, K. Raghavachari, A. Rendell, J. C. Burant, S. S. Iyengar, J. Tomasi, M. Cossi, N. Rega, J. M. Millam, M. Klene, J. E. Knox, J. B. Cross, V. Bakken, C. Adamo, J. Jaramillo, R. Gomperts, R. E. Stratmann, O. Yazyev, A. J. Austin, R. Cammi, C. Pomelli, J. W. Ochterski, R. L. Martin, K. Morokuma, V. G. Zakrzewski, G. A. Voth, P. Salvador, J. J. Dannenberg, S. Dapprich, A. D. Daniels, Ö. Farkas, J. B. Foresman, J. V. Ortiz, J. Cioslowski, D. J. Fox, Gaussian 09, Revision E.01, Gaussian, Inc., Wallingford CT, **2013**.
- [69] M. D. Hanwell, D. E. Curtis, D. C. Lonie, T. Vandermeersch, E. Zurek, G. R. Hutchison, *J. Cheminf.* **2012**, *4*, 17.
- [70] C. Sikorska, T. Puzyn, *Nanotechnology*, **2015**, *26*, 455702.
- [71] H. Wang, Y. He, Y. Li, H. Su, *J. Phys. Chem. A*, **2012**, *116*, 255262.
- [72] N. Mardirossian, M. Head-Gordon, *Phys. Chem. Chem. Phys.* **2014**, *16*, 9904–9924.
- [73] R. D. Dennington II, T. A. Keith, J. M. Millam, GaussView 6.0.16, Semichem, Inc. 2000–2016.
- [74] T. Lu, F. Chen, *J. Comput. Chem.* **2012**, *33*, 580–592.
- [75] W. Humphrey, A. Dalke, K. Schulten, *J. Mol. Graph.* **1996**, *14*, 33–38.
- [76] M. F. Sanner, *J. Mol. Graphics Modell.* **1999**, *17*, 57–61.

RESEARCH ARTICLE

Entry for the Table of Contents



The combination of three privileged structures, fullerenes, selenosugars, and steroids, has led to new hybrids in which the novel methanofullerenes are decorated with fragments of biological interest. Theoretical calculations at the DFT-B3LYP-D3(BJ)/6-311G(2d,p) level allowed the determination of the most stable conformation, and docking simulations suggest the application of these compounds as potential inhibitors of the A β oligomerization.

Institute and/or researcher Twitter usernames: @UdeLaHabana